Iterative parameter estimation and model prediction of a rotary unmanned aerial vehicle

Rejina L.W. Choi

Mechatronics Research Laboratory,
Mechanical Engineering Department,
University of Canterbury,
Christchurch 8041, New Zealand
E-mail: rejina.choi@pg.canterbury.ac.nz

Christopher E. Hann*

Electrical and Computer Engineering Department,
University of Canterbury,
Christchurch 8041, New Zealand
E-mail: Chris.Hann@canterbury.ac.nz
*Corresponding author

XiaoQi Chen

Mechanical Engineering Department,
University of Canterbury,
Christchurch 8041, New Zealand
E-mail: xiaoqi.chen@canterbury.ac.nz

Abstract: This paper presents a method for identifying and predicting attitude dynamics in a rotary unmanned aerial vehicle (UAV). A base model which uses a first principles model is simplified for use in real-time prediction. An integral-based parameter identification method is presented to identify the unknown intrinsic helicopter parameters outdoors with significant wind disturbance and on a test bench. The yaw axis is used as a proof-of-concept on both the tests. For the outdoor flight, the system identification is performed using open-loop commands from a test pilot. The test-bench experiments use proportional integral derivative (PID) control and thus provide a further validation of the methods in closed-loop as well as open-loop. The results show that all the major yaw dynamics were captured and good future state predictions of 0.1 to 0.3 seconds were obtained using slow time varying parameters and disturbance modelling.

Keywords: UAV; unmanned aerial vehicle; minimal modelling; integral-based parameter identification, disturbance.

Reference to this paper should be made as follows: Choi, R.L.W., Hann, C.E. and Chen, X.Q. (2014) 'Iterative parameter estimation and model prediction of a rotary unmanned aerial vehicle', *Int. J. Intelligent Systems Technologies and Applications*, Vol. 13, Nos. 1/2, pp.81–102.

Biographical notes: Rejina L.W. Choi received her BSc in Electronic from Multimedia University and MSc in Embedded System from Heriot-Watt University, in 2006 and 2008 respectively. Currently, she is pursuing her PhD in the Department of Mechanical Engineering, Canterbury University, New Zealand. Her research interests are system identification and model predictive control.

Christopher E. Hann received first class BSc (Hons) 1996, and PhD 2001 in Mathematics from the University of Canterbury. Teaching fellow in the Mathematics Department until 2003, FRST postdoctoral fellow 2004–2006 and Sir Charles Hercus Health Research Fellow/Senior Research Associate 2007–mid 2010 in Mechanical Engineering. Lecturer in Department of Electrical Engineering mid 2010–2011, Senior Lecturer/Rutherford Discovery Fellow from 2012. His research areas include rocket systems and control, orbital mechanics, system identification and control for industry, biomedical systems, image processing and computer vision. He has published over 250 refereed papers and is an inventor on several patents.

XiaoQi Chen is a Professor in the Department of Mechanical Engineering at University of Canterbury. After obtaining his BE from South China University of Technology in 1984, he received China-UK Technical Cooperation Award for his MSc study in Department of Materials Technology, Brunel University (1985–1986), and PhD study in Department of Electrical Engineering and Electronics, University of Liverpool (1986–1989). He was Senior Scientist at Singapore Institute of Manufacturing Technology (1992–2006) and a recipient of Singapore National Technology Award in 1999. His research interests include mechatronic systems, mobile robotics, assistive devices, and manufacturing automation.

This paper is a revised and expanded version of a paper entitled ‘Minimal models to capture the dynamics of a rotary unmanned aerial vehicle’ presented at *M2VIP*, Auckland, 28–30 November, 2012.

1 Introduction

The control design of small-scaled helicopters is a challenging task. There are complicated high-order dynamics involved and thus a common approach uses the concept of linearised stability derivatives (Morris et al., 1994). Flight dynamics modelling typically linearises around operating regions for example hovering or forward flight (Mettler et al., 2000). Parameters can be identified directly using state space identification method and Extended Kalman Filter (Salman et al., 2006; Kallapur and Anavatti, 2006; Lyashevskiy and Yaobin, 1996; Song et al., 2010). However, they often require good initial estimates of states and require time for convergence which may not always be available or suitable during flight since even at the hovering speeds, wind disturbances can change the angle of attack and thus the helicopter could move in and out of the pre-tuned operating region. This paper presents a real time, time varying modelling methodology which involves accounting for disturbances during flight and allows attitude dynamics to be updated over short periods to lump the effects of unmodelled dynamics.

The paper is motivated by flight of remote control (RC) helicopters outdoors where parameters are constantly influenced by wind disturbance and complex flows across the helicopter. In other words, model based control design which depends on a static model of helicopter would not perform well without accounting for the changing parameters in the underlying model as well as disturbance. Current methods that have been used to estimate online parameters of helicopter dynamics heavily rely on offline helicopter dynamics as a starting point. One of the methods is based on recursive least square (RLS) (Raptis et al., 2009), of which the performance depends on the persistency of excitation signal to avoid windup in covariance matrix that causes the lost of tracking capability (Vahidi et al., 2005). Another approach relies heavily on offline estimation of the parameters value as initial condition, for neural-network based online parameters estimation (Kenné et al., 2006). However, online training of neural-network is vey computationally expensive so has limited use in real-time and still has the issue of require reasonable convergence time which is not suitable for fast transient periods that would occur during windy and turbulent conditions. This paper investigates the possibilities of using a time-varying parameter model and disturbance estimation to improve the prediction capabilities of a static model, which could be used to improve control. Some experimental tests are carried out in full outdoor flight as well as using a test rig indoors to further investigate the algorithm without the added wind disturbance.

The paper is organised as follows. In Section 2, the model structure is presented. Section 3 describes an iterative integral-based parameter identification methodology for time-varying parameters as well as an analytical prediction method. Section 4 gives the experimental set up and Section 5 presents the experimental and simulation results comparison and discussion. The conclusion and future work is presented in Section 6.

2 Model structure

The small scale helicopter is modelled using the standard equation:

$$\dot{\boldsymbol{\omega}}^B = \mathbf{I}^{-1}(\mathbf{I}\boldsymbol{\omega}^B \times \boldsymbol{\omega}^B) + \mathbf{I}^{-1}\boldsymbol{\tau}^B, \tag{1}$$

where $\boldsymbol{\omega}^B = [p \quad q \quad r]^T$ is the angular velocity in body fixed reference frame, $\boldsymbol{\tau}^B = [M_\phi \quad M_\theta \quad M_\psi]$ is the moment components along body axes,

$$\mathbf{I} = \begin{pmatrix} I_{xx} & 0 & -I_{xz} \\ 0 & I_{yy} & 0 \\ -I_{xz} & 0 & I_{zz} \end{pmatrix}, \tag{2}$$

is the fuselage inertial matrix in body coordinates. A reduced form of the model from (Kim and Tilbury, 2004) is used in the experiment in this paper. Denoting $\dot{\phi} = p$, $\dot{\theta} = q$ and $\dot{\psi} = r$, the overall roll, pitch and roll dynamics are defined:

$$\dot{p} = k_1 qr + k_2 \delta_\theta - k_3 p + k_4 q + k_{d,1} \tag{3}$$

$$\dot{q} = k_5 pr + k_6 \delta_\phi - k_7 q - k_8 p + k_{d,2} \tag{4}$$

$$\dot{r} = k_9 pq + k_{10} \delta_\psi - k_{11} r - k_{12} \delta_o + k_{d,3} \tag{5}$$

where,

$$k_1 = \frac{(I_{yy} - I_{zz})}{I_{xx}}, \quad k_2 = \frac{P_m}{I_{xx}}\left(\frac{\alpha_3 L_3 L_8}{L_9} + C_1\right),$$
$$k_3 = \frac{P_m}{I_{xx}}\left(\frac{\alpha_4 L_1 (L_2 + L_3)}{\Omega} + C_2\right), \quad k_4 = \frac{P_m}{I_{xx}} C_3 \tag{6}$$

$$k_5 = \frac{(I_{zz} - I_{xx})}{I_{yy}}, \quad k_6 = k_2, \quad k_7 = k_3, \quad k_8 = \frac{P_m}{I_{yy}} C_3 \tag{7}$$

$$k_9 = \frac{(I_{xx} - I_{yy})}{I_{zz}}, \quad k_{10} = \frac{n}{2} a_T c_T \rho \pi {R_T}^3 {\Omega_T}^2 \frac{B^3}{3}, \quad k_{11} = K_g, \quad k_{12} = K_m \tag{8}$$

$$P_m = \frac{n \rho a c \Omega^2 R^4 B^4}{16 L_1 (L_2 + L_3)} \tag{9}$$

The parameters k_1, k_6 and k_{10} are considered as the torque constant from the main and tail rotor blade; k_3, k_7 and k_{11} are the overall effective damping; $k_{d,1}$, $k_{d,2}$ and $k_{d,3}$ are added as constant external torque offset modelling asymmetry in the roll, pitch and yaw axes respectively; α_3, α_4 is a correction factor to compensate for simplified aerodynamics, $L_{1,2,3,4}$ are the linkage lengths in rotor hub assembly, ρ is the air density, Ω is the main rotor angular velocity, l is the position along the main rotor blade, and a is the main rotor lift slope, is the main blade chord length and is the main rotor aerodynamics lift element. Assuming constant value in ρ, a, c, c_1, the time constant of the pitch and roll of the helicopter are proportional to rotation speed of the main rotor.

The servo actuator dynamics are an important subsystem that indirectly link to rigid body dynamics. It is commonly modelled as first order system:

$$\dot{\theta}_{\text{cyc}} + \tau \theta_{\text{cyc}} = k \delta_{\text{cyc}} \tag{10}$$

where θ_{cyc} is the blade pitch angle, τ is time constant, k is input gain constant and $\delta_{\text{cyc}} \in \delta_\phi, \delta_\theta, \delta_\psi$. The servo actuator dynamics time constant partially contributed to the time delay of the helicopter attitude response to the cyclic control input. In the simulation environment, the time delay e^{-Ts} is approximated using Pade approximation in form of rational function and the pure time delay T value is chosen by finding the optimal correlation between the commanded angle and the measured attitude response.

3 Time varying parameters and disturbance model formulation for yaw dynamics

This paper presents the methods on yaw dynamics to demonstrate the concept but it is equally applicable to all axes. The yaw model of equation is further simplified by setting the inertial term to zero and assuming the rotor torque gain is constant, which yields the model:

$$\text{model}_{\text{static}} \equiv \dot{r} = -k_1 r + k_2 (\delta_\psi + k_d) \tag{11}$$

Equation (11) is a static model of the system where k_d is assumed to be constant for all time and is the baseline model for comparison in this paper. To allow for changes in k_1 and k_2 and the model external disturbance, equation (11) is rewritten in the form:

$$\dot{r} = -k_1(t)r + k_2(t)(\delta_\psi(t) + k_{\text{offset}}(t) + u_d(t)) \tag{12}$$

where $k_{\text{offset}}(t)$ models the asymmetry in the helicopter which will capture any steady state offset and $u_d(t)$ models fast frequency external disturbance. The parameters $k_1(t), k_2(t)$ and $k_{\text{offset}}(t)$ are allowed to change over time but at much slower frequency than $u_d(t)$. Define:

$$\begin{aligned} T_{\text{slow}} \equiv\ & \text{time period where the intrinsic parameters} \\ & k_1, k_2 \text{ and } k_{\text{offset}} \text{ are approximately constant} \end{aligned} \tag{13}$$

$$T_{\text{fast}} \equiv \text{time period where the disturbance } u_d(t) \text{ is approximately constant} \tag{14}$$

Assume that $T_{\text{slow}} \gg T_{\text{fast}}$ and define the time period:

$$I_{\text{slow},t_o} = \{[t_o - T_{\text{slow}}, t_o], t_o > T_{\text{slow}}\} \tag{15}$$

For $t \in I_{\text{slow},t_o}$ define the model:

$$\text{model}_{\text{slow}} \equiv \dot{r} = -k_{1,o}r + k_{2,o}(\delta_\psi + k_{\text{offset},o}),\ t \in I_{\text{slow},t_o} \tag{16}$$

where:

$$k_{1,o} \equiv k_1(t_o),\ k_{2,o} \equiv k_2(t_o),\ k_{\text{offset},o} \equiv k_{\text{offset}}(t_o) \tag{17}$$

are assumed unknown parameters.

From equation (13), $k_1(t) \simeq k_{1,o}, k_2(t) \simeq k_{2,o},\ k_{\text{offset}}(t) \simeq k_{\text{offset},o}$ for $t \in I_{\text{slow},t_o}$. Since the $k_{\text{offset}}(t)$ term in equation (12) effectively ensures that the mean of the disturbance $u_d(t)$ is 0, the yaw dynamics of equation (16) approximate the yaw dynamics of equation (12).

The next step is to identify the fast frequency disturbance $u_d(t)$ in equation (11). For the given time t_o, define:

$$I_{\text{fast},t_o} = \{[t_o - T_{\text{fast}}, t_o], t_o > T_{\text{slow}}\} \tag{18}$$

By definition of T_{fast} in equation (14), $u_d(t)$ is constant for $t \in I_{\text{fast},t_o}$ thus the yaw dynamics in this time period can be approximated by the model:

$$\text{model}_{\text{fast}} \equiv \dot{r} = -\hat{k}_{1,o}r + \hat{k}_{2,o}(\delta_\psi + \hat{k}_{\text{offset},o} + u_{d,o}), t \in I_{\text{fast},t_o} \tag{19}$$

where:

$$u_{d,o} \equiv u_d(t_o) \tag{20}$$

is assumed to be an unknown parameter and $\hat{k}_{1,o}, \hat{k}_{2,o}$ and $\hat{k}_{\text{offset},o}$ are assumed to be estimated in prior step in equation (11).

3.1 Iterative integral method-intrinsic parameters

For any given interval I_{slow,t_o} in equation (15), the goal is to identify the parameters $k_{1,o}, k_{2,o}$ and $k_{\text{offset},o}$ in equation (16) given measured yaw rate data $r(t)$ and the control input $\delta_\psi(t)$ during this time period. An integral method first developed in Hann et al. (2008) and Docherty et al. (2011) is significantly extended to handle the high frequency sampling rate in this helicopter application.

Firstly, the interval I_{slow,t_o} is partitioned into n equally spaced intervals, $\{[T_{i-1}, T_i],\ i = 1,\ldots n\}$. Integrating equation (16) from T_{i-1} to t yields:

$$\begin{aligned} r(t) - r(T_{i-1}) = &-k_{1,o}\int_{T_{i-1}}^{t} r \,\mathrm{d}t + k_{2,o}\int_{T_{i-1}}^{t} \delta_\psi \,\mathrm{d}t \\ &+ k_{2,o}k_{\text{offset},o}(t - T_{i-1}), \quad t \in [T_{i-1}, T_i),\ i = 1,\ldots,n \end{aligned} \tag{21}$$

Let $r_{\text{data,slow}}(t)$ denote the measured yaw rate data on I_{slow,t_o}, set $r_{\text{approx}}(t) = r_{\text{data,slow}}(t)$ and define the piecewise function:

$$\begin{aligned} r_{\text{model}}(t) &= r_{o,1} - k_{1,o}\int_{T_o}^{t} r_{\text{approx}}(t)\,\mathrm{d}t + k_{2,o}\int_{T_o}^{t} \delta_\psi \,\mathrm{d}t + \bar{k}_{\text{offset},o}(t - T_o) \\ &= \cdots \\ &\vdots \\ &= r_{o,n} - k_{1,\text{o}}\int_{T_{n-1}}^{t} r_{\text{approx}}(t)\,\mathrm{d}t + k_{2,o}\int_{T_{n-1}}^{t} \delta_\psi \,\mathrm{d}t + \bar{k}_{\text{offset},o}(t - T_{n-1}) \end{aligned} \tag{22}$$

where:

$$\begin{aligned} &r_{o,i} = r_{\text{data,slow}}(T_{i-1}), \quad i = 1,\ldots,n, \\ &\bar{k}_{\text{offset},o} = k_{2,o}k_{\text{offset},o} \end{aligned} \tag{23}$$

Note that the piecewise formulation of equations (22) and (23) ensures that disturbances modelling error and noise do not cumulatively increase over time to swamp the solution by 'resetting' the model to the measured data at each interval $[T_{i-1}, T_i]$.

The parameters $k_{1,o}, k_{2,o}$ and $\bar{k}_{\text{offset},o}$ are found by fitting $r_{\text{model}}(t)$ in equation (22) to the measured yaw rate data $r_{\text{data,slow}}(t)$ by standard linear regression. Define the resulting parameters:

$$\begin{aligned} \left\{\hat{k}_{1,o}, \hat{k}_{2,o}, \hat{\bar{k}}_{\text{offset},o}\right\} \equiv &\text{ parameters } k_{1,o},\ k_{2,o},\ \bar{k}_{\text{offset},o} \text{ obtained by linear regression} \\ &\text{of equation (22) on the data } r_{\text{data,slow}}(t),\ t \in I_{\text{slow},t_o} \end{aligned} \tag{24}$$

A new approximation $r_{\text{approx}}(t)$ to the data is then obtained by substituting $k_{1,o} = \hat{k}_{1,o}$, $k_{2,o} = \hat{k}_{2,o}, \bar{k}_{\text{offset},o} = \hat{\bar{k}}_{\text{offset},o}$ into equation (22). This new $r_{\text{approx}}(t)$ is put again into the integrand of equation (22) and the updated $r_{\text{mod}el}(t)$ is used to obtain a new set of parameters $\hat{k}_{1,o}, \hat{k}_{2,o}, \hat{\bar{k}}_{\text{offset},o}$ in equation (24) by linear regression. This process is continued until convergence. The overall algorithm is summarised in Figure 1.

Figure 1 Algorithm of Integral method

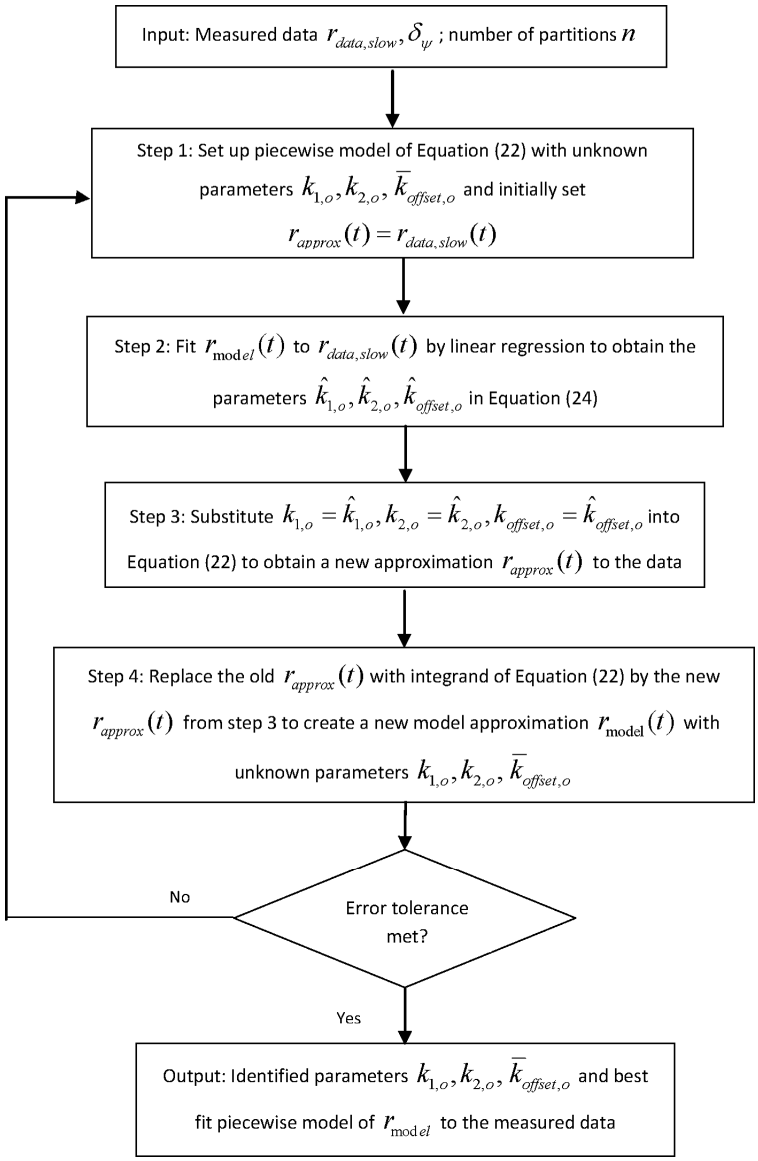

3.2 Integral method: disturbance

Once the intrinsic parameters $k_{1,o}, k_{2,o}$, $\overline{k}_{\text{offset},o}$ are identified in equation (16) these parameters are substituted into equation (19) and thus the only unknown to identify is $u_{d,o}$. Since this is a small interval, modelling error does not have sufficient time to build up, hence a simpler non-iterative method can be used. Equation (19) is first integrated from T_o to t, which yields:

$$r(t) = r_o - \hat{k}_{1,o}\int_{T_o}^{t} r \, \mathrm{d}t + \hat{k}_{2,o}\int_{T_o}^{t} (\delta_{\psi} + k_{\text{offset},o}) \, \mathrm{d}t + \hat{k}_{2,o} u_{d,o}(t - T_o), \quad t \in I_{\text{fast},t_o} \tag{25}$$

Let $r_{\text{data,fast}}(t)$ denote the measured yaw rate data on I_{fast,t_o} and define the function:

$$r_{\text{model,fast}}(t) = r_o - \hat{k}_{1,o}\int_{T_o}^{t} r_{\text{data,fast}}\,\mathrm{d}t + \hat{k}_{2,o}\int_{T_o}^{t}(\delta_\psi + \hat{k}_{\text{offset},o})\,\mathrm{d}t + \overline{u}_{d,o}(t - T_o) \tag{26}$$

where:

$$\overline{u}_{d,o} = \hat{k}_{2,o}u_{d,o} \tag{27}$$

The parameter $\overline{u}_{d,o}$ is found by fitting $r_{\text{model,fast}}(t)$ to the measured data by linear regression, and the $u_{d,o}$ can be determined from equation (27) since $\hat{k}_{2,o}$ is known. In summary, the identified disturbance is defined:

$$\begin{aligned}\hat{u}_{d,o} \equiv\ &\text{Disturbance from fitting } r_{\text{model,fast}} \text{ in equation (26)}\\ &\text{to the measured data by linear regression}\end{aligned} \tag{28}$$

3.3 Model prediction

The three models of equations (11), (16) and (19) are now compared by predicting ahead a given time period T_{fast}. A prediction is made at every available data point and the residual errors between the model prediction and the actual measured value are collected for further analysis. The predictions at a time point $t = t_o$ are obtained by solving equation (16) analytically in Malple, which yields:

$$r_{\text{soln}}(t) = r_o\mathrm{e}^{-\hat{k}_{1,o}(t-t_o)} + \hat{k}_{2,o}\int_{t_o}^{t}\mathrm{e}^{-\hat{k}_{1,o}\times(t-z)}(\delta_\psi(z) + \hat{k}_{\text{offset},o} + u_{d,o})\,\mathrm{d}z \tag{29}$$

After some simplification, the three model predictions are thus defined:

$$\begin{aligned}&\text{Static prediction} \equiv r_{\text{soln,static}}(t_o + T_{\text{fast}})\\ &\qquad = (r_o - k_d)\mathrm{e}^{-k_1(T_{\text{fast}})} + k_d + k_2\int_{t_o}^{t_o+T_{\text{fast}}}\mathrm{e}^{-k_1\times(t-z)}\delta_\psi(z)\,\mathrm{d}z\end{aligned} \tag{30}$$

$k_1, k_2, k_d \equiv$ Static parameters from equation (11).

$$\begin{aligned}&\text{Slow prediction} \equiv r_{\text{soln,slow}}(t_o + T_{\text{fast}})\\ &\qquad = (r_o - \hat{k}_{\text{offset},o})\mathrm{e}^{-\hat{k}_{1,o}(T_{\text{fast}})} + k_{\text{offset},o} + \hat{k}_{1,o}\int_{t_o}^{t_o+T_{\text{fast}}}\mathrm{e}^{-\hat{k}_{1,o}\times(t-z)}\delta_\psi(z)\,\mathrm{d}z\end{aligned} \tag{31}$$

$\hat{k}_{1,o}, \hat{k}_{2,o}, \hat{k}_{\text{offset},o} \equiv$ Slow time-varying parameters which are constant over I_{slow,t_o}.

$$\begin{aligned}&\text{Fast prediction} \equiv r_{\text{soln,fast}}(t_o + T_{\text{fast}})\\ &\qquad = (r_o - \hat{k}_{\text{offset},o} - \hat{u}_{d,o})\mathrm{e}^{-\hat{k}_{1,o}(T_{\text{fast}})} + \hat{k}_{\text{offset},o} + \hat{u}_{d,o}\\ &\qquad\quad + \hat{k}_{1,o}\int_{t_o}^{t_o+T_{\text{fast}}}\mathrm{e}^{-\hat{k}_{1,o}\times(t-z)}\delta_\psi(z)\,\mathrm{d}z\end{aligned} \tag{32}$$

$\hat{k}_{1,o}, \hat{k}_{2,o}, \hat{k}_{\text{offset},o} \equiv$ Slow time varying parameters which are constant over I_{slow,t_o}.

$\hat{u}_{d,o} \equiv$ Equation (28).

4 Experimental setup

4.1 Model helicopter

A scaled model helicopter Trex 600 ESP is used for data collection in an outdoor flight. It is equipped with Bell-Hiller stabilizer bar that increase the stability of the helicopter by providing damping on pitch and roll response. With a two-bladed rotor of 0.6 m radius and high torque brushless motor, it has payload capacity of 2 kg which allow it to carry the instrumentation equipments and flying for about 15 minutes.

The Trex 450 SE remote control (RC) helicopter is smaller in size compared to Trex 600 SE and is chosen as the platform for carrying out experiments on test rig to demonstrate and validate the minimal modelling and system identification methods of this paper. It is equipped with Bell-Hiller stabiliser bar and has a two-bladed rotor of about 0.3 m radius.

4.2 Test rig

A test rig was built for the RC helicopter so that indoor experiments can be carried out in safe manner and to allow individual axes in the helicopter to be isolated (Weilenmann and Geering, 1994). It also allows validation of the parameter identification method without the significant disturbance from the wind outdoors, and is thus an intermediate step to bridge the gap to full flight. Figure 2 shows the helicopter test set up with the test rig. The test rig was built to have 4 degrees of freedom (DOF) which are the three attitude axes and vertical displacement. The pitch and roll angle on the rig are limited to –40° to 40°, while the maximum vertical displacement is 40 cm.

Figure 2 Helicopter test rig

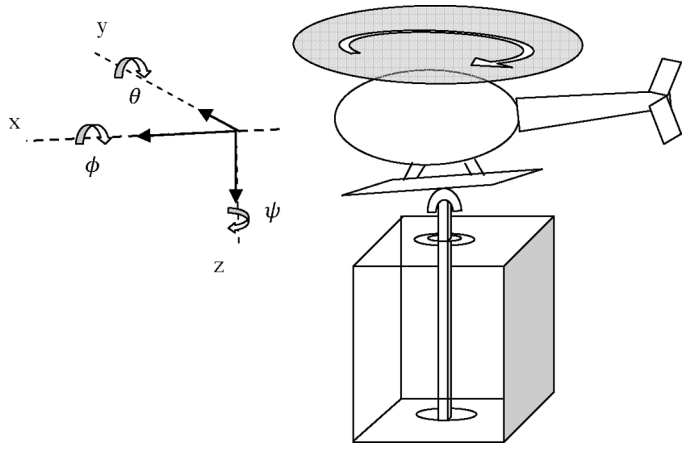

Attitude information is read from a low cost 9 degree of freedom (DOF) razor inertial measurement unit (IMU) to Arduino Due microcontroller board at a sampling rate of 50 Hz. The microcontroller board is also used for reading the helicopter actuation input which are the pulse width signal for four servo motors. The four servo motors provide the actuation input to the helicopter. Three of the motors are arranged in 120 degrees around a swash plate so that each servo motor can elevate one side of swash plate and their

combined efforts represent the cyclic and collective pitch input command of the helicopter. The last servo motor is for adjusting the tail rotor blade pitch angle and has a direct link to the pedal input command of the helicopter.

In order to correlate the control inputs to the four servos pulse width modulation (PWM) signal, an experiment is performed assume the linear correlation:

$$\begin{bmatrix} U_{\text{AILE}} \\ U_{\text{AUX}} \\ U_{\text{ELEV}} \\ U_{\text{RUDD}} \end{bmatrix} = G \times \begin{bmatrix} \delta_\phi \\ \delta_\theta \\ \delta_o \\ \delta_\psi \end{bmatrix} \tag{33}$$

where $\begin{bmatrix} U_{\text{AILE}} & U_{\text{AUX}} & U_{\text{ELEV}} & U_{\text{RUDD}} \end{bmatrix}^T$ are the four servo motor signals pulse width measurement, $\begin{bmatrix} \delta_\phi & \delta_\theta & \delta_o & \delta_\psi \end{bmatrix}^T$ are the pilot sticks adjustment range (±1 for $\delta_\phi, \delta_\theta, \delta_\psi$ and δ_o). After substituting the obtained data from a few combinations of control input with a corresponding PWM signal, the resulting formula is obtained:

$$\mathbf{U} = \mathbf{G}' \times \delta + \mathbf{U}_{\text{trim}} \tag{34}$$

where $\mathbf{U}_{\text{trim}}$ is the pulse width for starting position of pilot stick position, $\mathbf{G}'$ is the determined control input gain. In order to access the control input at any time, the following equation translates the servo motors pulse width to the corresponding control input:

$$\delta = \mathbf{G}'^{-1}(\mathbf{U} - \mathbf{U}_{\text{trim}}) \tag{35}$$

In addition, the microcontroller is interfaced with a Bluetooth transceiver modem BlueSMiRF Silver for sending and receiving information to and from the helicopter wirelessly within a distance of approximately 18 m. The microcontroller board acts as a relay for information passing between helicopter and a computer via Bluetooth signal and data logging is done on a computer.

5 Results

The system identification methods of Figure 1 and of equations (11)–(20), and the model prediction approach of equations (29)–(32) is tested on both outdoor free flying helicopter data and the test rig of Figure 2. For the outdoor data, significant wind disturbance was present which provides a good test case for the effectiveness of the fast prediction of equation (32) and the identified disturbance which in this case would directly capture the effect of wind gusts. These wind gusts will change the angle of attack and provide turbulent translational movement which would change the lift coefficient and damping over time, so that the time varying parameter model of equation (12) is ideally suited to this situation. The data analysed on this outdoor data is the yaw axis so it can be directly contrasted with the yaw axis on the test rig. Note that yaw is the most freely available axis that can be easily decoupled experimentally from the roll and pitch axes. Of particular interest is the comparison between the three models of equations (11), (16) and (19) in particular the effect of adding disturbance into the model prediction. Finally, some basic proportional derivative (PD) control results are presented on the test rig to

show how effective the minimal modelling and system identification methods are at capturing closed loop responses in contrast to the open loop inputs from the pilot in the outdoor helicopter data. It also shows the ability to predict the responses of a different set of gains that was not used to tune the original model including the input of real time disturbance identification on prediction. The main motivation behind these comparisons is to justify the use of simplified models for real-time implementation on the helicopter which is future work.

5.1 System identification and model prediction of outdoor helicopter data

Experimental data was obtained by a number of manual manoeuvres executed by a test pilot via a remote control system. Sinusoidal low frequency excitations were performed on the yaw axis in the presence of significant wind disturbance. Figure 3(a) shows the yaw rate over a 30 s run with the control pedal given in Figure 3(b).

The algorithm of Figure 1 is now applied to identify the static parameters of the yaw response in Figure (a), which yields:

$$k_1 = 3.546\ \mathrm{s}^{-1},\ k_2 = 777.50\ \mathrm{deg\ s}^{-2}\ /\ u_{\mathrm{ped}},\quad k_{\mathrm{offset}} = 27.869\,\mathrm{deg\,s}^{-2} \tag{36}$$

$$\text{median error} \equiv 0.1147\ \text{deg/s},\quad 90\%\ \text{confidence interval(CI)} \equiv [-12.12\ 11.77]\ \text{deg/s} \tag{37}$$

The parameters in equation (36) form the baseline static model for comparison with the model prediction approaches of equations (16) and (19).

The next step is to apply the slow updating model of equation (16) to characterise the improvements on model prediction. Firstly, to investigate the effect of the time period T_{slow} in equation (13), several values of 5, 10, 15 s are chosen with a prediction interval of $T_{\mathrm{fast}} = 0.1$ s. For example with $T_{\mathrm{slow}} = 5$ s, starting at $t_o = 5$ s, the algorithm of Figure 1 is applied to identify $k_{1,o}, k_{2,o}$ and $\overline{k}_{\mathrm{offset},o}$ and then these values are used to predict the future yaw at $t = 5.1$ s using the analytical formula of equation (31). The sampling period is 0.02 s so this calculation is repeated for $t = 5.02$, 5.04, 5.06, … The residuals of all the predictions are stored and the results are given in Table 1 including a comparison with the predictions from the static model using the parameters of equations (30) and (36). To further see these results visually, Figure 4 overlays the predicted values with the measured values for both the static and slow model cases.

The result shows that the major dynamics are captured and the discrepancies are due to unmodelled dynamics which can be further improved with time varying parameter identification. The result from Table 1 shows that $T_{\mathrm{slow}} = 10$ s is the optimal value for lowest model error. For the T_{slow}=15 s, the model error is higher compared to 10 s which indicates that this interval is not sufficiently short to capture some of the fast changing disturbance acting on the helicopter. The yaw rate error for all three values of T_{slow} is significantly lower than the yaw rate error for the static model, as expected since the static model cannot react to changes in the attitude dynamics. This significant improvement demonstrates that the wind is having a significant effect on the attitude parameters over time.

Figure 3 (a) Measured yaw rate data and (b) control pedal input (see online version for colours)

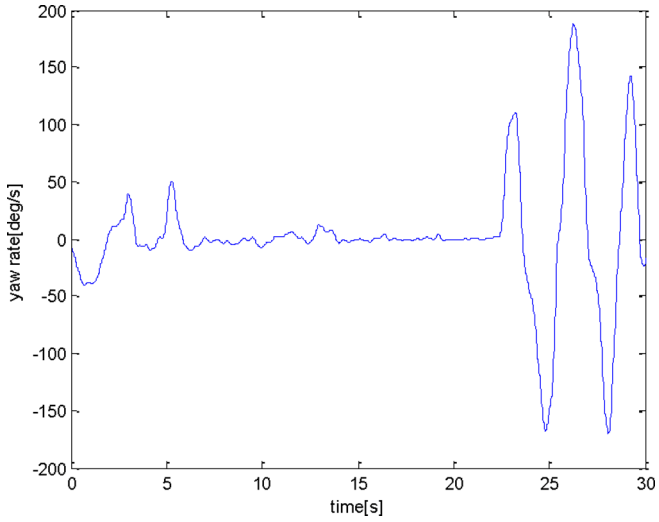

(a)

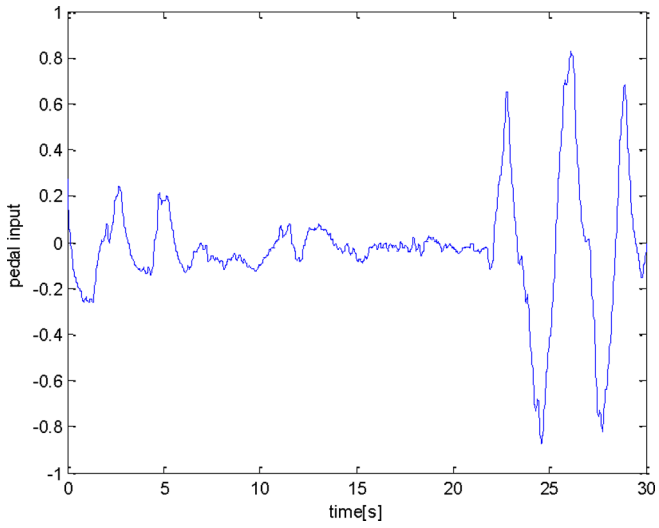

(b)

Table 1 Predictions of the slow model for several values of T_{slow} and T_{fast} = 0.1 s

	Yaw rate error (*slow model*)		*Yaw rate error* (*static model*)	
T_{slow} (s)	*Median* (deg/s)	*90% CI* (deg/s)	*Median* (deg/s)	*90% CI* (deg/s)
5	0.1018	[–5.7211 7.6100]	0.1147	[–12.12 11.77]
10	0.0155	[–5.3370 6.8334]		
15	0.2082	[–6.1265 7.4097]		

The effect of the disturbance identification and prediction with equations (25)–(28) and equation (32) is now investigated. A value of $T_{\text{slow}} = 10$ s is chosen so initially $t_o = 10$ s and a moving window of 10 s is shifted across all the data in a similar way to Table 1, but with three different prediction intervals of $T_{\text{fast}} = 0.1$, 0.2, 0.3 s. The results are given in Table 2 and the predicted vs. measured value are given in Figure 5.

It can be seen that the 90% CI is significantly reduced with $T_{\text{fast}} = 0.1$ s and the errors are comparable to Table 1 even for the larger prediction times of 0.2 and 0.3 s. This ability to accurately predict forward will enable model-based control to be used in future work.

As a further comparison, the static model parameters from equation (36) are used instead of updating the $k_{1,o}, k_{2,o}$ and $\overline{k}_{\text{offset},o}$. Disturbance is identified and the yaw rate is predicted forward for $T_{\text{fast}} = 0.1$, 0.2 and 0.3 s in a similar way to Table 2. The results are given in Table 3.

Table 2 Predictions of the fast model for several values of T_{fast}

	Yaw rate error (deg/s)	
T_{fast} (s)	*Median* (deg/s)	*90% CI* (deg/s)
0.1	0.0501	[–4.0006 4.9103]
0.2	0.0635	[–5.0578 6.3018]
0.3	0.1278	[–6.1279 7.5973]

Figure 4 (a) Prediction results for static model and (b) prediction results for slow model (see online version for colours)

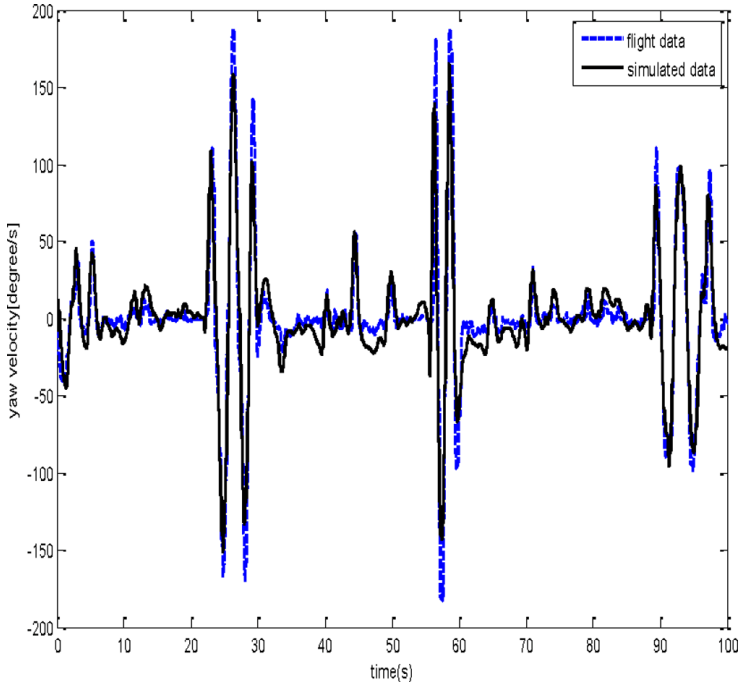

(a)

Figure 4 (a) Prediction results for static model and (b) prediction results for slow model (see online version for colours) (continued)

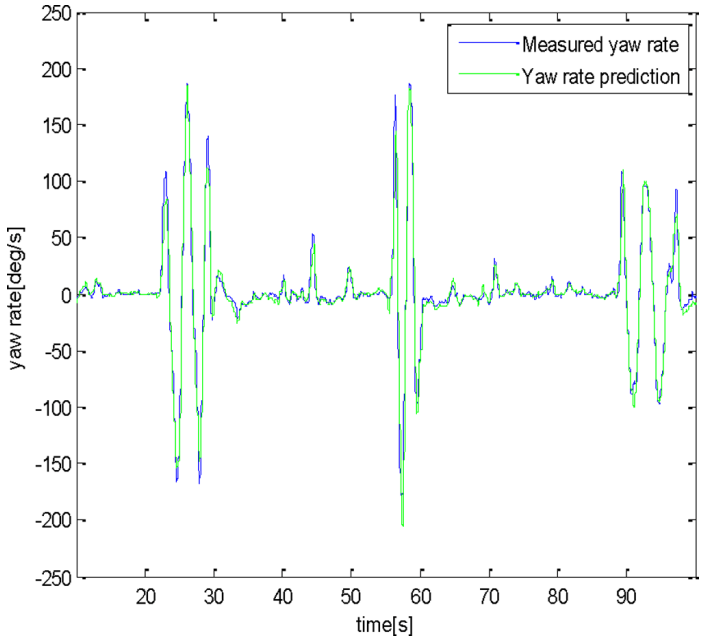

(b)

Figure 5 Prediction results for fast model (see online version for colours)

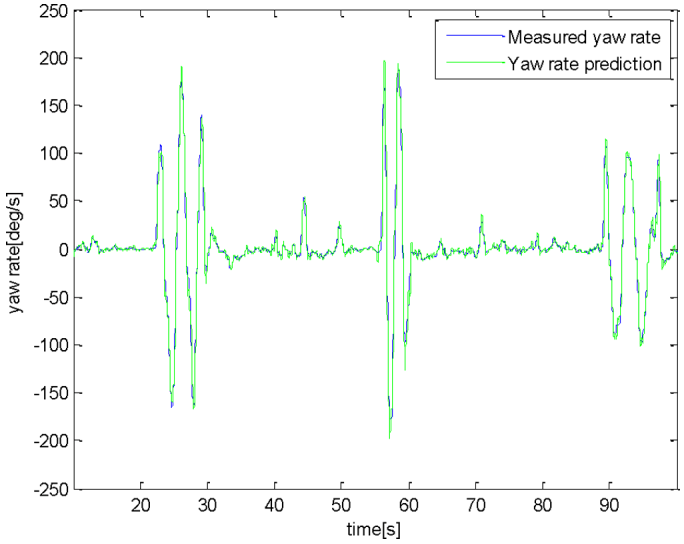

Interestingly, the results of Table 3 are quite similar to Table 2. The reason is that the slow time-varying parameters will be lumped into this fast time-varying disturbance. However, the advantage of the method of Table 2 is that no prior knowledge of the helicopter is required, where in Table 3 a static model must be available.

Table 3 Prediction of fast model based on static model

	Yaw rate error (deg/s)	
T_{fast} (s)	*Median* (deg/s)	*90% CI* (deg/s)
0.1	0.0666	[–4.5720 4.7029]
0.2	0.0603	[–6.0017 5.8924]
0.3	0.1503	[–6.7178 6.8084]

5.2 System identification and model prediction of test rig data

To further test the algorithm of Figure 2, a PD controller on the yaw angle is implemented with a gain of $K_p = 0.01$ and $K_d = 0.001$. Note that an infinite impulse response (IIR) low pass filter is implemented on the yaw angle data to reduce the effect of measurement noise. One source of the measurement noise is from the vibration of the helicopter frame which was picked up by the accelerometer in the IMU. This vibration is only translational so should have minimal effect on the yaw angle, however the accelerometer is part of the data fusion in the sensor's Kalman filter to reduce the drift so the weighting from this vibration causes unwanted noise in the yaw angle. Figure 6 shows a step response for a PD controller based on taking direct data from the sensor which has a lot of oscillation. To reduce this sensor noise an IIR low pass filter is implemented with 15 Hz cutoff frequency. Figure 7 shows another step response with same gain after applying the filter, which shows a considerable improvement.

Note that an alternative solution to the filter which will give a much improved result would be to buy a much more expensive sensor for example a laser gyro. However, for a basic proof of concept the cheaper IMU is adequate and has the advantage that it is low cost so is easily replaced.

The underlying model for a PD controller is defined:

$$\dot{r} = -k_1 r + k_2(\delta_\psi + k_d) \tag{38}$$

$$\delta_\psi(t) = K_p(r_o - \int_0^t r) + K_d(-r) \tag{39}$$

$$\begin{aligned} &r_o \equiv \text{reference yaw angle,} \\ &K_p, K_d \equiv \text{proportional(P) and derivative(D) gains} \end{aligned} \tag{40}$$

A similar method to Figure 1 is used to identify the parameters k_1, k_2 and k_d and are assumed constant throughout, since there is no wind disturbance on the test rig indoors. The only difference is that δ_ψ in equation (22) is no longer fixed throughout all the iterations but updated in step 4 of Figure 1 by substituting $r_{\text{approx}}(t)$ into the r value in equation (39) which then goes into equation (22). Figure 8 shows the result of the yaw and yaw rate.

There is significant steady state error in Figure 8(b), but this is due to the yaw rate being matched without knowledge of the yaw angle. This steady state angle is easily accounted for by decrease the offset angle to –12° which is the mean value after steady state which is approximately 3 s. Figure 9(a) and (b) show the yaw rate and angle after the adjustment.

Figure 6 Yaw response without filtering (see online version for colours)

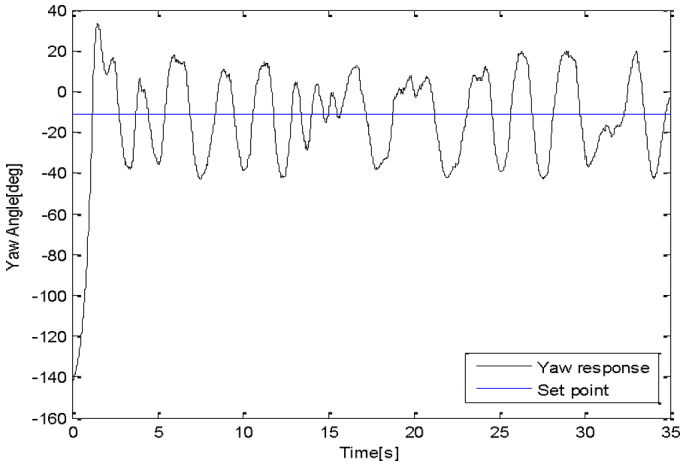

Figure 7 PD control ($K_p = 0.01$, $K_d = 0.001$) yaw response with filtering (see online version for colours)

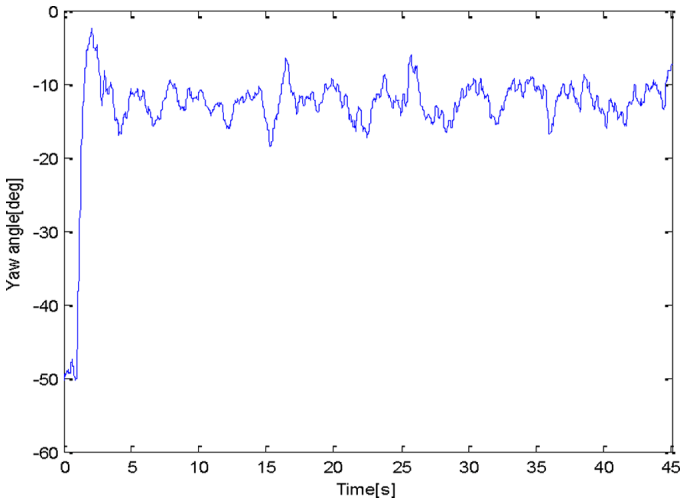

There is a minimal change in the yaw rate, but the steady state error is now captured. The remaining error is predominantly due to the sensor error in the yaw angle which is significantly magnified by the controller. To account for this the model predictive method of equation (32) is used with $T_{\text{fast}} = 0.1$ s. The new curve is given in Figure 10.

Both the yaw rate and yaw angle are predicted very accurately with this method demonstrating the potential for using this model in real real-time to improve the control response. A further experiment is now performed with $K_p = 0.02$, $K_d = 0.001$, $K_i = 0.01$. The same parameters are used from the first experiment and the resulting static model with the second experiment control input is used to predict the yaw response. Figure 11 shows the results. Using the identified parameters of the first experiment, the fast model prediction method of equation is used to predict the yaw angle. The prediction interval is chosen to be $T_{\text{fast}} = 0.1$ s. The resulting prediction vs. measured data is given in Figure 12.

Figure 8 (a) Modelled vs. experiment yaw rate for PD control on test rig and (b) modelled vs. experiment yaw angle for PD control on test rig (see online version for colours)

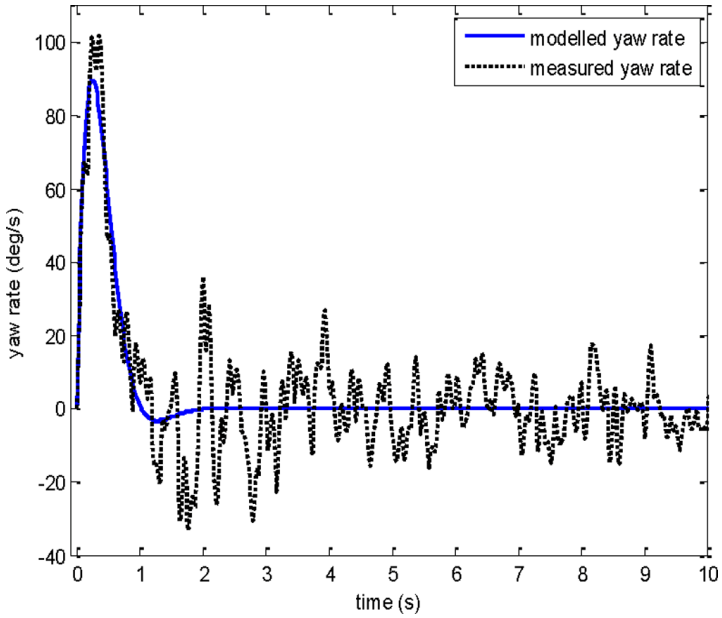

(a)

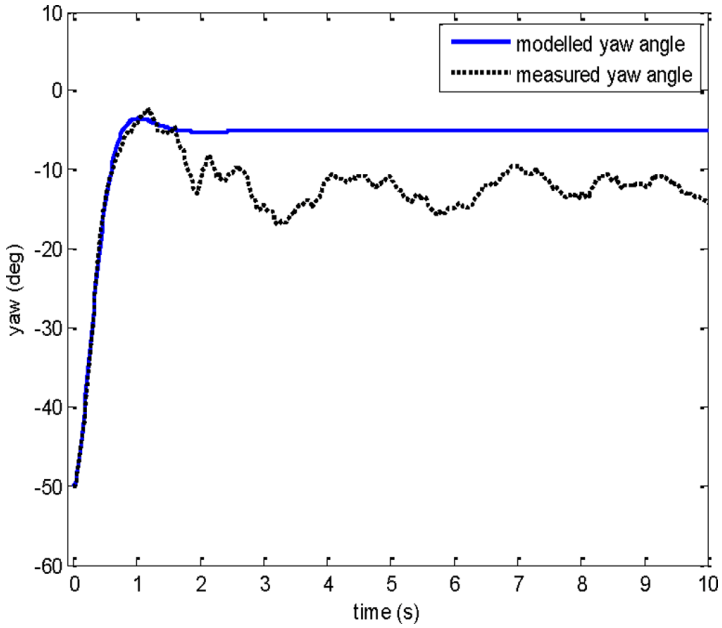

(b)

Figure 9 (a) Modelled vs. experiment yaw rate after adjustment and (b) modelled vs. experiment yaw angle after adjustment (see online version for colours)

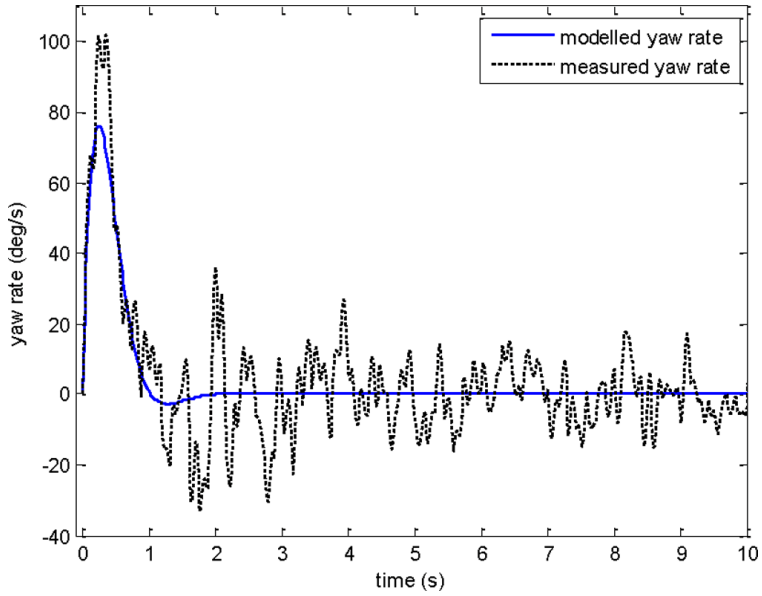

(a)

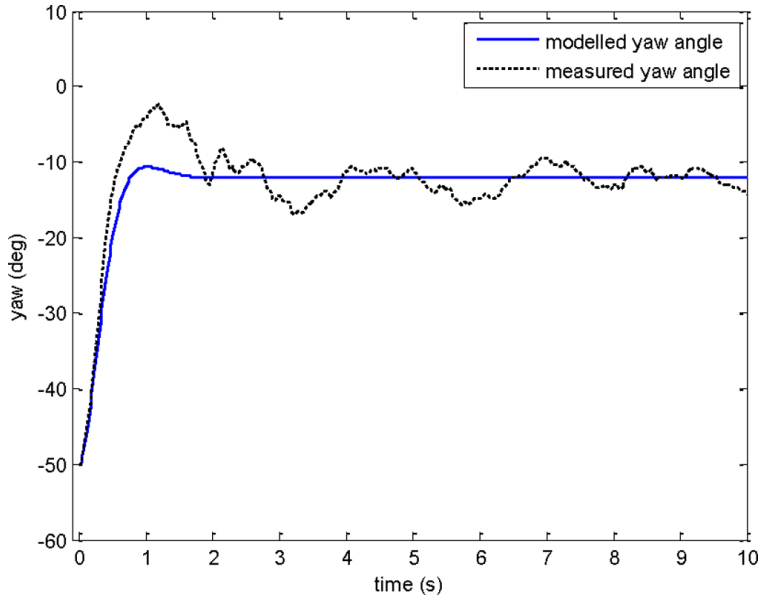

(b)

Figure 10 PD yaw angle with disturbance prediction (see online version for colours)

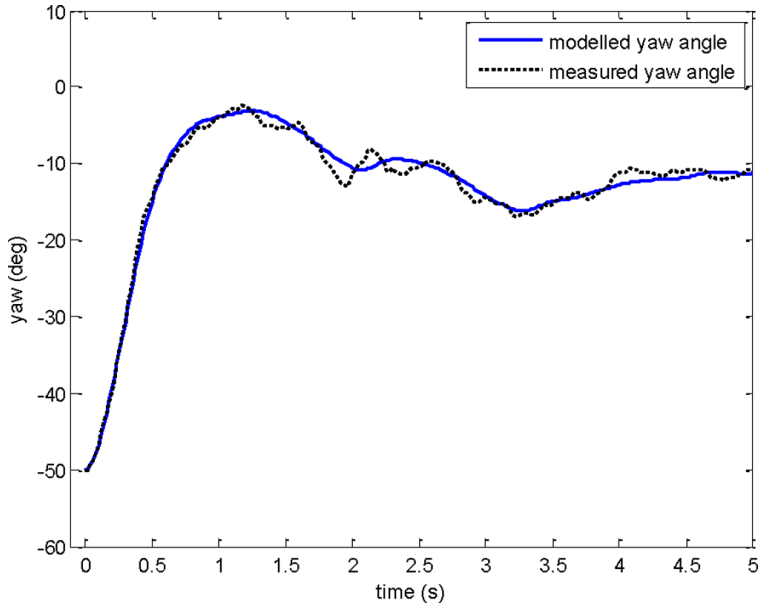

Figure 11 (a) Modelled vs. experiment yaw rate for PID control and (b) modelled vs. experiment yaw angle for PID control (see online version for colours)

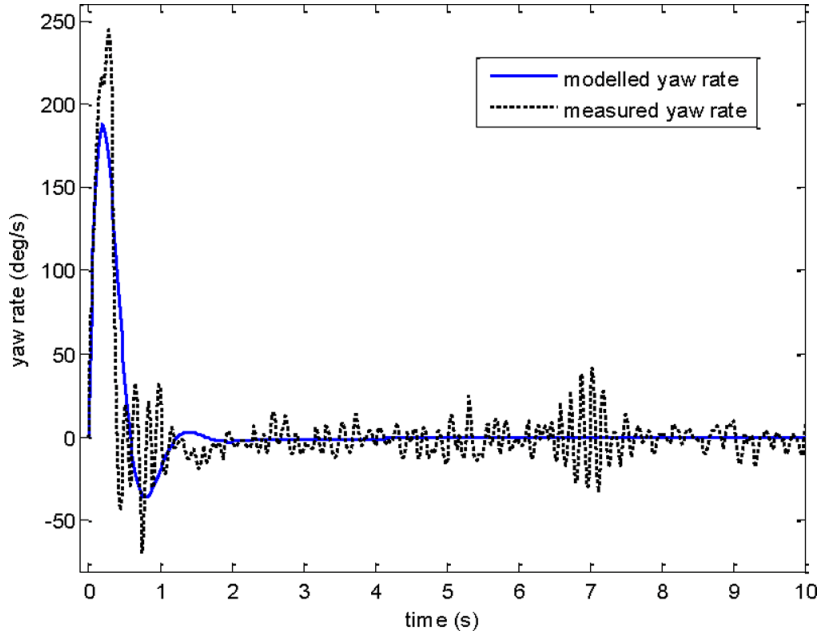

(a)

Figure 11 (a) Modelled vs. experiment yaw rate for PID control and (b) modelled vs. experiment yaw angle for PID control (see online version for colours) (continued)

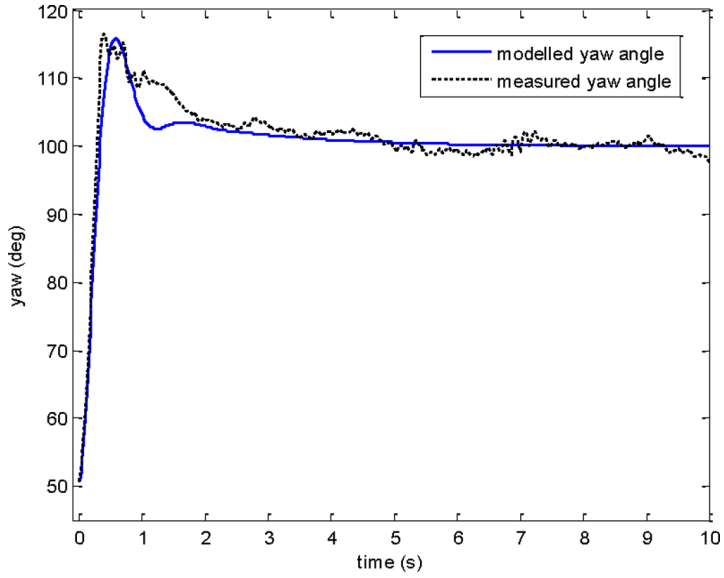

(b)

Figure 12 PID yaw angle with disturbance prediction (see online version for colours)

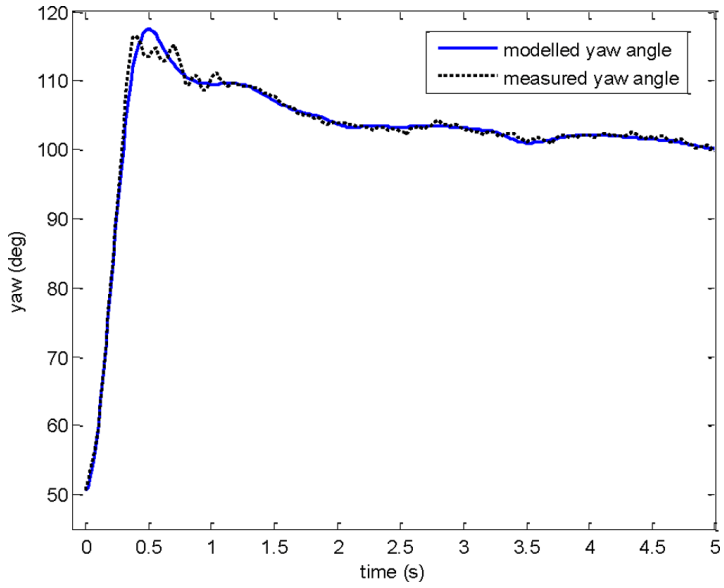

6 Conclusion

A minimal modelling and iterative integral-based parameter estimation method is presented for capturing the dynamics of a model helicopter for both outdoor flight and an

indoor test rig. A complex 6DOF model was reduced into a set of simplified models including a decoupled yaw model which was used to prove the concepts. The yaw axis was chosen since it was the easiest to mechanically isolate on the test rig.

The outdoor data contained significant wind disturbances which change the angle of attack and create translational dynamics which will affect the attitude dynamics. This effect was captured by having a combination of slow time-varying intrinsic parameters, and a fast time-varying disturbance which models for example wind gusts. The iterative integral method worked very well and required very minimal computational effort. To validate the models a predictive approach was used. That is, a given section of data was used to tune the parameters, and future data was predicted by assuming these parameters remained constant into the future. Hence, with this method, there is no guarantee that a model with more parameters would necessarily give better prediction.

An optimum slow identification interval where the helicopter's intrinsic parameters are assumed constant, was found to be 10 s and combined with a fast identification interval of 0.1 s to capture disturbance, gave the best results. However, the combination of a static model and a fast identification interval of 0.1 s gave slightly worse but reasonably comparable results. This result suggests that with offline identification to create an initial static helicopter model, a real-time disturbance identification algorithm would be sufficient to account for modelling error and wind disturbance in flight. This option would be much easier to implement on a chip as there would be no large matrix inversions required, which is needed to identify the slow time-varying helicopter parameters in real-time. However, since the iterative integral method only requires integrals of the data and linear least squares it could also be potentially implemented on a chip in future work. The advantage of a real-time method is that if conditions change so that the static model is significantly inaccurate, then there is capability for automatically adapting during flight. Future work will investigate this issue.

Another significant advantage with this work is that the predictions are done by analytically solving the differential equations. Hence, the expressions can be pre-stored to allow very fast computation in real-time. One simple application of the real-time system identification would be to calculate the required constant actuation angle δ_ψ in equation (39) that would take an initial non-zero yaw rate to 0 at a future time interval, for example 0.1 s. This required angle could be analytically solved in Maple, so would be easily calculated on a chip. This angle can be updated every time step and would thus function as a yaw rate controller.

The test rig has proven to be a good intermediate step to flight and allows simple testing of algorithms before implementation outdoors. It can also be tethered to a computer so there are no issues with computation in the proof-of-concept stage. A basic static model with PD and PID control worked well to predict the test rig response. The iterative integral method was also proven to be capable of identifying dynamics in closed-loop as well as open-loop. Specifically, given an experimental test with $K_p = 0.01$ and $K_d = 0.001$, a static model was derived that gave very good overall prediction of a $K_p = 0.02$, $K_d = 0.001$, $K_i = 0.01$ response. Combined with the disturbance identification, this approach is very effective in predicting non-linear helicopter response with quite simple models, so could allow significant improvements in control, which is left for future work.

References

Docherty, P.D., Chase, J.G., Lotz, T.F., Hann, C.E., Shaw, G.M., Berkeley, J.E., Temorenga, L., Mann, J.I. and Mcauley, K. (2011) 'Independent cohort cross-validation of the real-time DISTq estimation of insulin sensitivity', *Comput. Methods Prog. Biomed.*, Vol. 102, pp.94–104.

Hann, C.E., Chase, J.G., Ypma, M.F., Elfring, J., Nor, N.M.H., Lawrence, P. and Shaw, G.M. (2008) 'The impact of parameter identification methods on drug therapy control in an intensive care unit', *The Open Medical Informatics Journal*, Vol. 2, pp.92–104.

Kallapur, A.G. and Anavatti, S.G. (2006) 'UAV linear and nonlinear estimation using extended Kalman filter', *Computational Intelligence for Modelling, Control and Automation, 2006 and International Conference on Intelligent Agents, Web Technologies and Internet Commerce, International Conference on*, 28 November–1 December, 2006, p.250.

Kenné, G., Ahmed-Ali, T., Lamnabhi-Lagarrigue, F. and Nkwawo, H. (2006) 'Nonlinear systems parameters estimation using radial basis function network', *Control Engineering Practice*, Vol. 14, pp.819–832.

Kim, S.K. and Tilbury, D.M. (2004) 'Mathematical modeling and experimental identification of an unmanned helicopter robot with flybar dynamics', *Journal of Robotic Systems*, Vol. 21, pp.95–116.

Lyashevskiy, S. and Yaobin, C. (1996) 'Nonlinear identification of aircraft', *Control Applications, 1996, Proceedings of the 1996 IEEE International Conference on*, 15–18 September, 1996, pp.327–331.

Mettler, B., Kanade, T. *et al.* (2000) 'System identification modeling of a model-scale helicopter', *Journal of the American Helicopter Society*.

Morris, J.C., Van Nieuwstadt, M. and Bendotti, P. (1994) 'Identification and control of a model helicopter in hover', *American Control Conference*, Vol. 2, 29 June–1 July 1994, pp.1238–1242.

Raptis, I., Valavanis, K. and Moreno, W. (2009) 'System identification and discrete nonlinear control of miniature helicopters using backstepping', *Journal of Intelligent and Robotic Systems*, Vol. 55, pp.223–243.

Salman, S.A., Puttige, V.R. and Anavatti, S.G. (2006) 'Real-time validation and comparison of fuzzy identification and state-space identification for a UAV platform', *Computer Aided Control System Design, 2006 IEEE International Conference on Control Applications, 2006 IEEE International Symposium on Intelligent Control, 2006 IEEE*, 4–6 October, 2006, pp.2138–2143.

Song, B., Mills, J.K., Liu, Y. and Fan, C. (2010) 'Nonlinear dynamic modeling and control of a small-scale helicopter', *International Journal of Control, Automation, and Systems*, Vol. 8, pp.534–543.

Vahidi, A., Stefanopoulou, A. and Peng, H. (2005) 'Recursive least squares with forgetting for online estimation of vehicle mass and road grade: theory and experiments', *Vehicle System Dynamics*, Vol. 43, pp.31–55.

Weilenmann, M.F. and Geering, H.P. (1994) 'Test bench for rotorcraft hover control', *Journal of Guidance, Control, and Dynamics*, Vol. 17, pp.729–736.